Scientific Research Publishing

Materials Sciences and Applications, 2022, 13, 107-131
https://www.scirp.org/journal/msa
ISSN Online: 2153-1188
ISSN Print: 2153-117X

Preparation and Properties of pH-Responsive Intelligent Medical Dressing Based on Bacterial Cellulose/Polyacrylic Acid

Fei Jiang, Wen Zhang*, Siyu Guo, Xin Zhang

Shaanxi University of Science & Technology, Xi'an, China
Email: *zwen102@163.com

How to cite this paper: Jiang, F., Zhang, W., Guo, S.Y. and Zhang, X. (2022) Preparation and Properties of pH-Responsive Intelligent Medical Dressing Based on Bacterial Cellulose/Polyacrylic Acid. *Materials Sciences and Applications*, **13**, 107-131.
https://doi.org/10.4236/msa.2022.133008

Received: February 23, 2022
Accepted: March 25, 2022
Published: March 28, 2022

Abstract

Bacterial cellulose/polyacrylic acid (BC/PAA) pH-responsive hydrogels were prepared by free-radical polymerization (*in situ*) using BC as the raw material and AA as the monomer. The hydrogels were loaded with curcumin (Cur) to prepare pH-responsive intelligent medical dressings. The preparation process of the hydrogels was optimized by a single factor and response surface experiment using their swelling degree as an index. The structures of BC/PAA pH-responsive hydrogels were characterized by scanning electron microscope (SEM), Fourier Transform Infrared spectrometer (FTIR), X-ray diffraction (XRD), and tensile tester, and the swelling properties, mechanical properties, bacteriostatic properties, and drug release behavior were investigated. The results showed that the BC/PAA pH-responsive hydrogel has a three-dimensional network structure with the swelling rate up to 1600 g/g, compressive strength of up to 8 KPa, and good mechanical properties, and the drug release behavior was in line with the logistic dynamics model, and it has good inhibitory effects on common pathogens of wound infection: *E. coli*, *S. aureus,* and *P. aeruginosa.*

Keywords

Bacterial Cellulose, Polyacrylic Acid, *In Situ* Polymerization, pH-Responsive Hydrogel, BC/PAA-Cur Intelligent Medical Dressing

1. Introduction

A hydrogel is an interpenetrating three-dimensional network structure material with good swelling and biocompatibility. Environmentally responsive [1] hy-

*Corresponding author.

drogels, a class of hydrogels that change the drug release pattern by adjusting environmental physicochemical parameters, such as pH, temperature, and ionic strength, have received a lot of attention in the field of controlled drug release [2] [3] [4], where the swelling behavior of pH-sensitive hydrogels can change with environmental pH and have been used successfully in targeted drug delivery systems in recent years [5] [6] [7]. pH-responsive hydrogels [1] contain hydrophilic groups, such as -OH, -CONH, -COOH, and $-SO_3H$, which endow the polymers with good water absorption properties. Meanwhile, these groups change the gel network structure (via protonation/deprotonation) and their swelling behavior, thereby enabling the polymers to guide drug release through a phase change or volume change under the change of the external environment. In an acidic environment, the hydrogel possesses a lower swelling rate, its structure remains compact, and the drug is "protected" inside the hydrogel. When the pH of the environment increases, the hydrogel further expands, thereby leading to drug release. This pH-responsive hydrogel can be invoked as a drug carrier for drug targeting release. For chronic bacterial infection wounds, the surface is weakly alkaline (pH > 7.3); however, when pH-responsive hydrogels are applied to such wounds, drugs can be made available at a faster rate, thus killing bacteria in a short time. However, in a wound with pus or necrotic tissue type (such as ulcers), its surface is acidic, which makes the hydrogels release the drug steadily and slowly [8].

Bacterial cellulose (BC) [9] is widely used in medical materials, such as trauma dressings [10], artificial blood vessels [11], drug carriers [12], artificial cartilage, and bone tissue scaffolds [13] due to its good biocompatibility and degradability. However, there are very few studies on the controlled release of pH-responsive herbal medicines for skin trauma. A previous study confirmed that BC-based hydrogels loaded with nano-arsenic have significant antibacterial, antioxidant, and anti-inflammatory properties and can be used as a topical dressing carrier for skin wound healing [14]. In addition, a study revealed that composites prepared by combining tannic acid and magnesium chloride with BC have good biocompatibility and that the antibacterial effect, when applied to infected wounds, is ideal [15]. Another study used BC-based hydrogels prepared by ionizing radiation as oral protein molecular carriers and found that the cumulative drug release in the simulated gastric fluid was less than 10%, which indicates the potential of these hydrogels to protect protein drugs from the gastric acid environment [16]. Furthermore, some authors use natural products as raw materials to develop hydrogels. A physical double network hydrogel prepared using natural glycyrrhizic acid and biocompatible polyvinyl alcohol in water/glycerol solvent demonstrated high mechanical properties, biocompatibility, and anti-freezing and anti-drying abilities [17]. A temperature-responsive cellulose hydrogel composite material (with cotton fiber as raw material), through a two-step polymerization of the temperature-responsive poly(N-isopropyl acrylamide) and polyurethane grafted onto fiber non-woven fabrics or with N,N-methylene double propylene copolymer grafted onto hydrogel carrier and its intelligent response regulation

behavior, is beneficial for applications in wound dressings and other fields [18]. Acrylic acid (AA) can form polyacrylic acid (PAA) under light, heat, or peroxide conditions [19]. PAA is a water-soluble electrolyte that contains a carboxyl hydrophilic group that can react to pH changes in the environment; it is a typical pH-sensitive hydrogel [20]. However, PAA has poor mechanical strength. Moreover, PAA hydrogels prepared by free radical polymerization have a small specific surface area and no pore structure, which makes the response rate late. AA and BC were compounded by *in situ* radical polymerizations to prepare BC/PAA pH-responsive hydrogels with a three-dimensional network structure. The hydrogels were used to load curcumin (Cur) in order to prepare intelligent medical dressings. Therefore, the optimal preparation process of the hydrogels was studied. The structure and properties of the hydrogels were characterized and tested by scanning electron microscopy (SEM), Fourier transforms infrared spectrometry (FTIR), X-ray diffraction (XRD), rotary rheometry, and servo-controlled high and low-temperature tensile testing in order to clarify the properties of the hydrogels. Furthermore, the pH-responsive drug release behavior and antibacterial performance of the intelligent medical dressings based on the hydrogels were investigated.

In this paper, we propose to prepare a BC/pH-responsive hydrogel-based smart medical dressing using BC as the dressing base and AA as the monomer. The dressing can overcome the defects of traditional medical gauze, absorb the wound exudate and toxin, block external infection source, prevent wound infection, good moisturizing and air permeability, easy to remove, no secondary damage to the wound, while intelligent response to wounding infection, the intelligent release of drugs loaded in the hydrogel when the wound becomes infected, thus inhibiting wound infection and promoting wound healing. This study can provide a foundation for the development of new medical dressings that have good economic and social benefits in the modern pharmaceutical industry.

2. Materials and Methods

2.1. Materials

Acrylic acid (AA), potassium persulfate ($K_2S_2O_8$), and N,N'-methylene bisacrylamide (MBA) were purchased from Damao Chemical Reagent Factory (Tianjin, China). Glycerol was purchased from Tianjin Fuyu Fine Chemical Co., Ltd. (Tianjin, China). BC membrane (purity ≥ 99.9%) was purchased from Hainan YIDA Food Industry Co., Ltd. (Hainan, China). Absolute ethanol (C_2H_5OH) was purchased from Tianjin Tianli Chemical Reagents Co., Ltd. (Tianjin, China). Phosphate-buffered saline (PBS, WH0112201 911XP), calcein-AM, and pyridinium iodide (PI) kit were purchased from Wuhan Procell Life Science & Technology Co., Ltd. (Hubei, China). Peptone, agar powder, beef paste, sodium dihydrogen phosphate, and potassium dihydrogen phosphate were purchased from Beijing Aoboxing Biology Technology Co., Ltd. (Beijing, China). Curcumin was purchased from Shanghai Yuanye Bio-Technology Co., Ltd. (Shanghai,

China). *E. coil*, *S. aureus*, and *P. aeruginosa* were purchased from Beijing Microbiological Culture Collection Co., Ltd. (Beijing, China).

2.2. Preparation and Process Optimization of BC/PAA pH-Responsive Hydrogels

The BC film was rinsed several times with deionized water and a neutral pH (pH 7) is reached. It was then soaked in 1 wt% NaOH solution at 60˚C for about 6 - 8 h. Afterward, the BC film was soaked in deionized water and refrigerated at 2˚C - 8˚C. Accurately, 6.30, 4.90, and 4.08 g BC films were suspended in 20 mL of deionized water and homogenized for 5 min with an adjustable high-speed homogenizer to form a uniform and stable dispersion. The monomer AA and the crosslinking agent MBA were added to make the final concentrations of 1 mol/L and 0.045 mol/L, respectively. The BC film was then placed in a 150 mL three-mouth flask and nitrogen was applied for 15 min. Potassium persulfate, an initiator relative to AA, was added and the reaction was stirred at 65˚C for 30 min. After the reaction, the reactants were injected into pre-warmed Petri dishes for 24 h, washed 3 - 4 times with deionized water at 60˚C, and freeze-dried at −60˚C for 12 h to obtain lyophilized BC/PAA pH-responsive hydrogels. BC/PAA pH-responsive hydrogels with m_{AA}/m_{BC} equivalent to 3:5, 1:2, and 3:7 prepared according to the above process and recorded as BC/PAA1, BC/PAA2, and BC/PAA3, respectively.

The swelling rate of the prepared hydrogel in the buffer solution (pH 8) was used as an index to investigate the influence of the following factors: 1) m_{AA}/m_{BC}: 1:1, 1:2, 1:3, 1:6, and 1:9; 2) reaction time: 15, 30, 45, 60, and 90 min; 3) reaction temperature: 50˚C, 55˚C, 60˚C, 65˚C, and 70˚C; 4) mass fraction of the cross-linker MBA: 0.025%, 0.045%, 0.065%, 0.085%, and 0.1%.

2.3. Structural Characterization and Performance Testing

Lyophilized BC membranes, PAA powders, and lyophilized BC/PAA pH-responsive hydrogels were analyzed by a VERTEX 70 Series FTIR spectrophotometer. The wavenumber range was 600 - 4000 cm^{-1}, the wavenumber accuracy was 0.01 cm^{-1}, and the resolution was better than 0.09 cm^{-1}.

The crystal structure of BC membrane PAA and freeze-dried BC/PAA pH-responsive hydrogels were analyzed by a D/max2200PC automatic X-ray diffractometer. The specification of this instrument is as follows: working voltage = 40 kV, current = 20 mA, λ = 0.154 nm, Cu target, Ni filter, scanning speed = 8˚/min, scanning range = 5˚ to 60˚, and step size 0.02˚.

FEI Verios460 scanning electron microscope was utilized to observe and photograph the freeze-dried BC film, PAA, and freeze-dried BC/PAA pH-responsive hydrogel after gold spraying.

The rheological properties of the hydrogels were investigated at the frequency range of 10 - 100 Hz using a HAAKE MARS 60 rotational rheometer. The diameter of the measurement plate was 25 mm, the measurement spacing was 1.5 mm, and the test temperature was constant at 25˚C. The storage modulus (G') and loss modulus (G") were also recorded.

The BC/PAA pH-responsive hydrogel was injected into a mold with a diameter of 1 cm and height of 1 cm to obtain a circular hydrogel with a diameter of 1 cm. The compression elastic modulus of the hydrogel sample was tested using a servo electronic tensile testing machine and the test rate was 2 mm/min. When the sample was compressed to 70% strain, the compression was stopped immediately and data were recorded.

The weight of the freeze-dried BC/PAA pH-responsive hydrogel with an m_{AA}/m_{BC} of 1:2 was denoted as W_d. The samples were plunged in a PBS buffer solution with pH 5.0, pH 6.0, pH 7.0, and pH 8.0 for 72 h, respectively, and the swelling equilibrium was reached. After wiping the surface of the samples, the weight was reported as W_s. The hydrogel swelling ratio (Q) was determined according to Formula (1):

$$Q = \frac{W_s - W_d}{W_d} \times 100 \tag{1}$$

where Q is the swelling rate (g/g), W_d and W_s is the mass of hydrogel before and after immersion (g), respectively.

The BC/PAA pH-responsive hydrogel was prepared by the optimal process that adopts the m_{AA}/m_{BC} of 1:2 and a round sample film of Φ2 cm was cut. The BC/PAA pH-responsive intelligent dressing was prepared by the adsorption method. In brief, 0.015 g Cur was dissolved in 5 mL ethanol and 2 g BC/PAA hydrogel was immersed in the Cur solution under dark conditions of 37˚C and 200 r/min oscillation for 24 h; the solvent was evaporated at room temperature.

The BC/PAA-Cur dressing (W_{total}) was sonicated in 10 mL of methanol for 8 min, centrifuged at 8000 rpm for 5 min, and the supernatant was obtained to determine its absorbance value at 425 nm in order to calculate the BC/PAA-Cur dressing loading W_1. Another BC/PAA-Cur dressing was placed in 500 mL of different media (Table 1) for drug release and the drug release solution was taken at 70, 80, 90, and 100 h. The Cur content in the solution was determined by spectrophotometry at 425 nm. The drug release rate (R_s) of the BC/PAA-Cur dressing was computed according to formula 2 and the drug release curve was drawn. The following four models were utilized: 1) zero-level release model: $Q = a + bx$; 2) Higuchi equation: $Q = bx^{1/2} + a$; 3) Logistic equation: $Q = a + (b-a)/(1+x/c)^d$; and 4) SWeibull equation: $Q = a - (a-b)e^{-(kx)^d}$ evaluation of BC/PAA-Cur dressing drug release behavior.

$$R_s(\%) = \frac{W_{total}}{W_1} \times 100 \tag{2}$$

Table 1. Drug release medium formulation.

	1#	2#	3#	4#	5#	6#	7#	8#
NaCl/(mol/L)	-	-	0.11	0.15	0.17	0.11	0.15	0.17
pH-buffer solution	4.0	8.0	4.0	4.0	4.0	8.0	8.0	8.0
Sodium dodecyl sulfate (%)	0.1	0.1	0.1	0.1	0.1	0.1	0.1	0.1

where W_1 is the mass of Cur in the drug release solution (mg); W_{total} is the drug loading of the BC/PAA-Cur dressing (mg).

Accurately, 2.0 g beef paste, 2.5 g peptone, and 7.5 g agar powder were weighed and dissolved in 500 mL of water. Their pH was adjusted to 7.2 - 7.4 to prepare an agar medium. The experimental equipment and culture medium were sterilized at 0.1 MPa and 121˚C for 20 min. The sterilized agar medium was prepared in Petri dishes under an aseptic environment and allowed to cool naturally until solidification. BC/PAA-Cur dressings containing 2, 3, and 6 wt% of Cur were prepared according to the method described in section 2.3.5, which were noted as BC/PAA-Cur2, BC/PAA-Cur3, and BC/PAA-Cur6, respectively. The BC/PAA pH-responsive hydrogel (φ15 mm, 3 mm thick) and the BC/PAA-Cur dressing were placed in a 24-well plate after UV irradiation for 12 h and 1 × 106 CFU/mL *E. coil* suspension (400 μL) was added. The antibacterial test of *S. aureus* and *P. aeruginosa* was consistent with the above steps.

1) Growth test

The above-mixed system was incubated at 37˚C for 48 h and then diluted to 10^{-4} - 10^{-6} CFU/mL. Accurately, 100 μL of the culture solution was evenly spread on nutrient agar plates and incubated at 37˚C for 48 h. The number of colonies was counted. The bacterial inhibition rate of the BC/PAA-Cur dressing was then calculated according to formula 3. The bacterial suspension without the addition of hydrogel was invoked as the control group.

$$\text{Antibacterial rate}(\%) = \frac{C_C - C_S}{C_C} \times 100 \tag{3}$$

where C_C is the average number of colonies in the control group and C_S is the average number of colonies in the sample group.

2) Evaluation of bacterial cell membrane integrity

The mixed system was incubated for 12 h at 37˚C. The hydrogel was removed and the remaining culture medium was centrifuged at 8000 rpm for 5 min; afterward, the cells were collected, resuspended, and stained with Calcein-AM and PI Live/Dead assay kit. The culture fluid was aspirated and the bacteria were resuspended on smears and observed under a Laser scanning Confocal Microscope (LSCM) at excitation and emission wavelengths of 494 nm and 514 nm, respectively.

The bacteria obtained by centrifugation after removing the hydrogel from the above-mixed system were fixed with 2.5% glutaraldehyde solution for 2 h, washed thrice with PBS, and dehydrated with 30%, 50%, 60%, 70%, 80%, and 100% ethanol in a graded manner (twice each, 15 - 20 min each time). The cell morphology of *E. coil*, *S. aureus*, and *P. aeruginosa* after subjection to sputtering gold spraying at 10 kV accelerating voltage was observed using SEM, respectively.

3. Results and Discussion

3.1. Preparation Process of BC/PAA pH-Responsive Hydrogel

The effect of m_{AA}/m_{BC} on BC/PAA pH-responsive hydrogel preparation is shown in **Figure 1(a)**. With the change of m_{AA}/m_{BC}, the hydrogel swelling rate showed

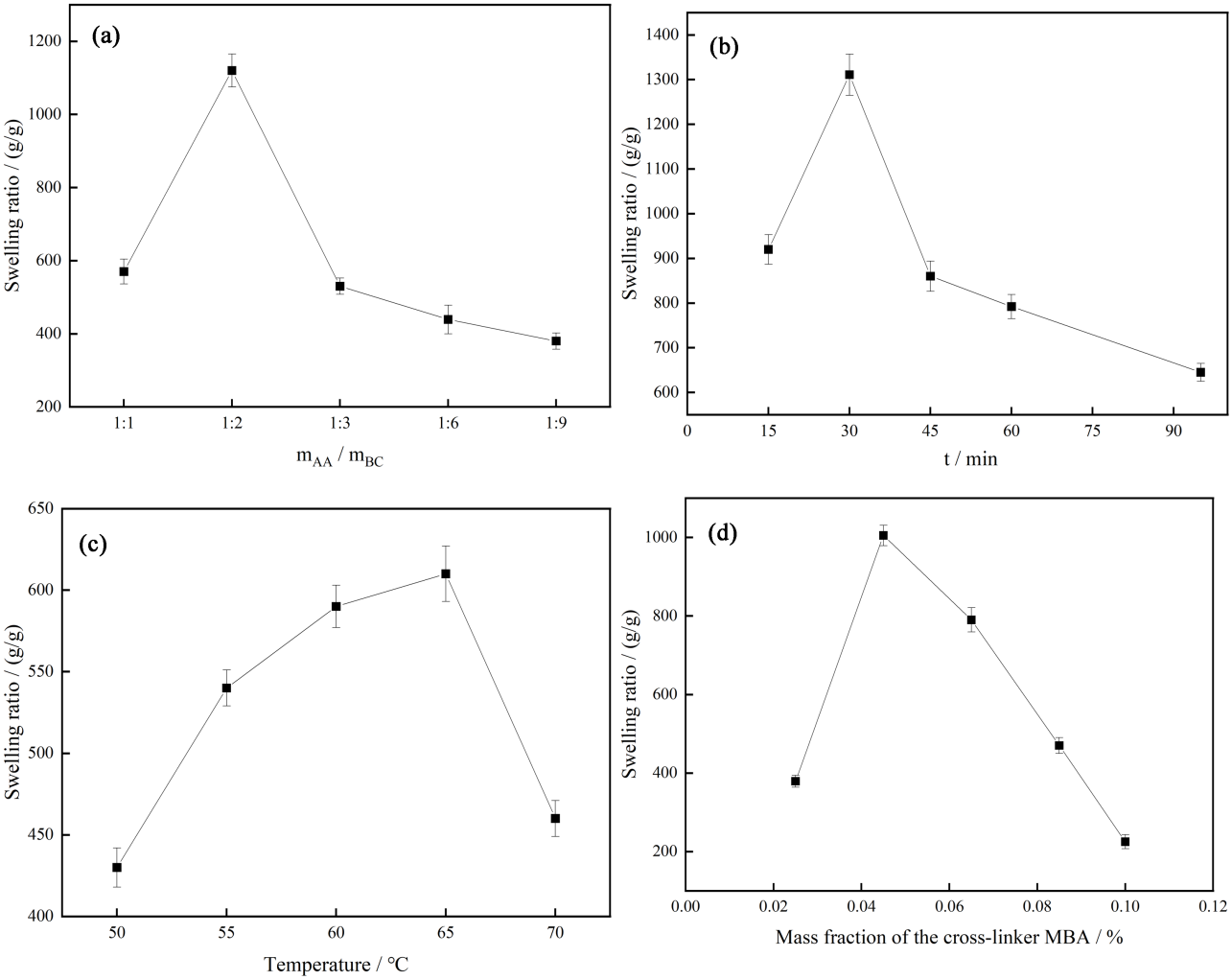

Figure 1. Effects of m_{AA}/m_{BC} (a), reaction time (b), reaction temperature (c), and addition of crosslinking agent (d) on the preparation of BC/PAA pH-responsive hydrogels.

an increasing trend, followed by a decreasing trend. The highest hydrogel swelling rate was observed when m_{AA}/m_{BC} was 1:2. This may be due to the interaction between BC and PAA during the polymerization reaction, which forms a certain network space and increases the water absorption of the hydrogel. The hydrogels prepared under different AA/BC mass ratios are transparent and soft blocks with certain elasticity and viscosity (**Figure 2**). With the increase of BC content, the color of the hydrogel gradually changed from transparent to milky white and the shading gradually increased as well. In addition, after adding BC, the texture of the hydrogel changed from soft to hard, showing a definite elasticity that may be due to the higher YounG's modulus and mechanical strength of BC. As depicted in **Figure 1(b)**, with an increase in the reaction time, the swelling ratio of hydrogels first increased gradually and reached the maximum value at 30 min. However, with the extension of the reaction time, the swelling ratio of hydrogels gradually decreased. This may be due to the fact that the polymerization time is too short. The polymer has not yet fully formed a three-dimensional network

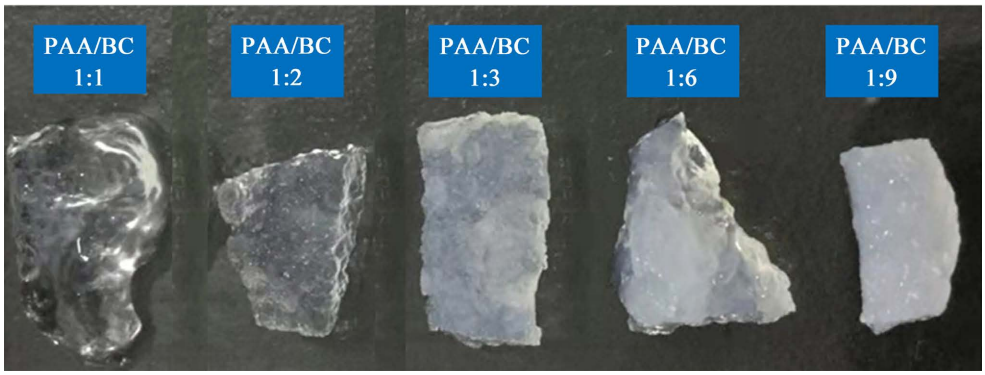

Figure 2. BC/PAA pH-responsive hydrogels with different mAA/mBC ratios.

structure and the water absorption performance of the hydrogels is not high. By extension of the reaction time, the polymer gradually formed a relatively complete three-dimensional network structure and the water absorption performance was improved. However, when the reaction time is too long, the molecular weight between the crosslinking sites is too small because of the intertwining effect of the larger molecular weight polydactyly acid chains and because the stretching of the network is restricted, which is not conducive to the transport of water molecules to the interior of the hydrogel, which in turn decreases the water absorption performance [21].

The effects of controlling other factors constant and changing the reaction temperature were investigated (**Figure 1(c)**). When the temperature was lower than 65˚C, the hydrogel swelling rate was small. This is because, at a lower temperature initiation reaction, the crosslinking rate is slow, which results in an incomplete reaction. Thus, it is difficult to form a good hydrogel network structure. However, when the reaction temperature reaches 65˚C, the swelling ratio of the hydrogel reaches the maximum. When the reaction temperature continues to increase, the polymerization rate is too fast and the speed of homopolymerization, chain initiation, and chain termination is also faster, which results in an uneven structure of the hydrogel and a low swelling ratio.

The effects of controlling other factors constant and changing the amount of cross-linking agents were investigated (**Figure 1(d)**). By increasing the dosage of the cross-linking agent, the hydrogel swelling rate showed a growing trend and then a decreasing trend, and the hydrogel swelling rate was maximum when the dosage of the cross-linking agent reached 0.045%. When the amount of cross-linking agent was less, the cross-linking density of the polymer was too low, thus forming a sparse three-dimensional network structure, which was not conducive to water retention. With the increase in the amount of the cross-linking agent, the crosslinking sites in the hydrogel network structure increased and the cross-linking density increased to form a network structure so that the hydrogel exhibits a good swelling property. When the amount of the crosslinking agent was too large, the hydrogel formed a sizable crosslinking density and a dense network structure, which weakened the water absorption performance and reduced

the swelling rate of the hydrogel. Therefore, 0.045% crosslinking agent was chosen as the optimal level for the preparation of hydrogels.

Based on the single factor experiment, the Box-Benhnken Design was used to conduct the response surface experiment on the BC/PAA pH response hydrogel preparation process. The experimental results were adjusted by statistical software to obtain a binary regression equation of the response value (Y) on the independent variable as follows: $A = 733 + 27.5A + 86.38B + 78.63C - 59AB + 185.5AC - 22.25BC - 77.88A^2 - 45.13B^2 - 93.13C^2$. Results of the regression ANOVA, as well as the significance analysis of this experimental model, are presented in Table 2.

The results showed that the R^2 of the model was 0.9337, which implies that 93.37% of the change in the response value is caused by independent variables (mass ratio, reaction time, and reaction temperature). This means that the change in the relationship between independent variables and dependent variables is obvious. The F value of the model was 10.96 ($p = 0.0023$), which indicates that the model was significant. The F value (lack of fit) of the equation was 0.89 ($p = 0.4816$) and the out-of-fit term was not significant. Therefore, the regression equation was well-fitted throughout the regression region. Thus, the points in the experiment can be replaced by this model and the experimental results can be analyzed. It can be seen that B, C, AC, A^2, and C^2 has a significant effect on the response values; therefore, there is no simple linear relationship between the dependent variables and the factors. The comprehensive analysis shows that for the response values, the mass ratio, reaction time, and reaction

Table 2. ANOVA of the response surface design of the experimental results.

Source of variance	quadratic sum	degree of freedom	F value	significance level*
model	351,157.69	9	10.96	0.0023
A-A	6050	1	1.69	0.2337
B-B	59,685.12	1	16.76	0.0046
C-C	49,455.12	1	13.8	0.0074
AB	13,924	1	3.9	0.0885
AC	137,641	1	38.64	0.0004
BC	1980.25	1	0.5559	0.4802
A2	25,534.8	1	7.2	0.0316
B2	8573.75	1	2.4	0.1647
C2	40,541.12	1	11	0.0119
residual	24,931.25	7		
lack of fit	10,637.25	3	0.89	0.4816
pure error	14,294	4		
summation	376,088.94	16		

temperature have a strong interaction effect on them.

Figure 3(a) showed that the swelling rate Q, which reflected the pH-responsiveness of the BC/PAA pH-responsive hydrogels, was extremely high when the mass ratio was 1:2; Q was also extremely high when the reaction temperature was 65˚C. With the change of the mass ratio and reaction temperature, the response value showed a gentle slope of a smooth surface, indicating that the interaction between factors A and B was relatively insignificant. Figure 3(b)

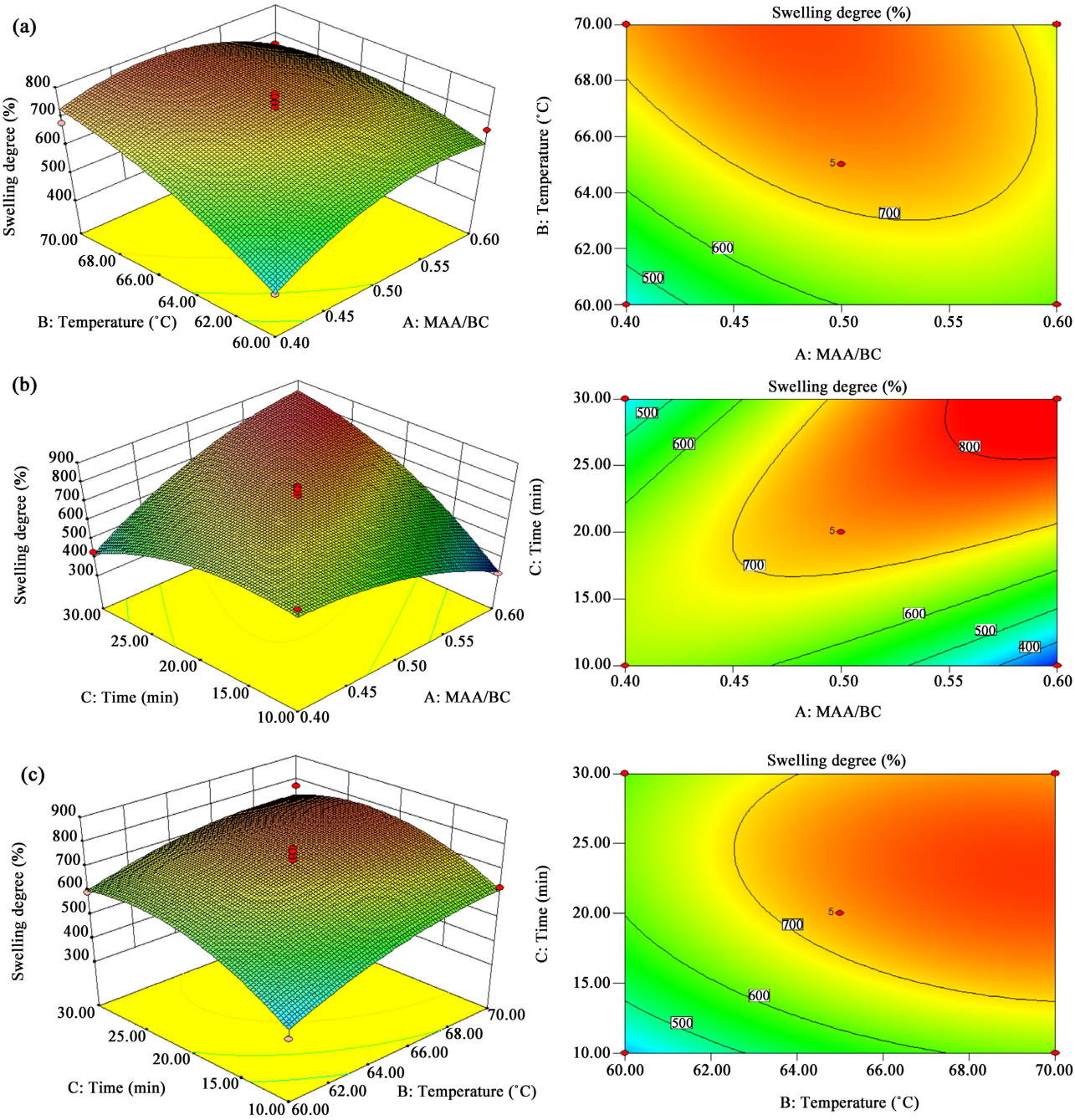

*p < 0.001 is considered highly significant; p < 0.05 is significant indigenous.

Figure 3. Response time contour and response surface diagrams.

showed that there was a great value of Q when the AA/BC mass ratio was 1:2 and that the response value was also maximum when the reaction time was 20 min. Meanwhile, the response surface was smooth and had a certain slope, which indicates that the interaction of factors A and C was more significant. Q was highest when the reaction temperature was 65˚C and the surface of the response surface was flattered at this time, which indicates that the interaction between factors B and C was less significant (**Figure 3(c)**). After analysis, the optimal preparation process of the BC/PAA pH-responsive hydrogel predicted by the regression model is as follows: AA/BC mass ratio of 1:2, a reaction time of 30 min, and reaction temperature of 65˚C. Under this process, the swelling rate of the BC/PAA pH-responsive hydrogel can reach 1600 g/g.

3.2. Characterization and Performance of BC/PAA pH-Responsive Hydrogel

As depicted in **Figure 4**, in the IR spectrum of BC [22], the vibration absorption peak of O-H was at 3347 cm^{-1}; the C-H stretching vibration absorption peak was near 2887 cm^{-1}, the -C=O- stretching vibration was near 1647 cm^{-1}; the absorption peak of the C-H bending vibration was close to 1429 cm^{-1} and 1321 cm^{-1}. The C-O stretching vibration was 1108 cm^{-1} and 1051 cm^{-1}. In the IR spectra of AA [23] [24], 3311 cm^{-1} was the stretching vibration of -OH in COOH; 1704 cm^{-1} was the -C=O stretching vibration; 1630 cm^{-1} was the characteristic absorption peak of C=C; the C-O stretching vibration was near 1250 cm^{-1}. In the IR spectrogram of BC/PAA, the -OH stretching vibration peak was at 3312 cm^{-1}; the -C=O stretching vibration was at 1702 cm^{-1}; the C-O stretching vibration was at 1241 cm^{-1}; the alcohol C-O stretching vibration was near 1040 cm^{-1},

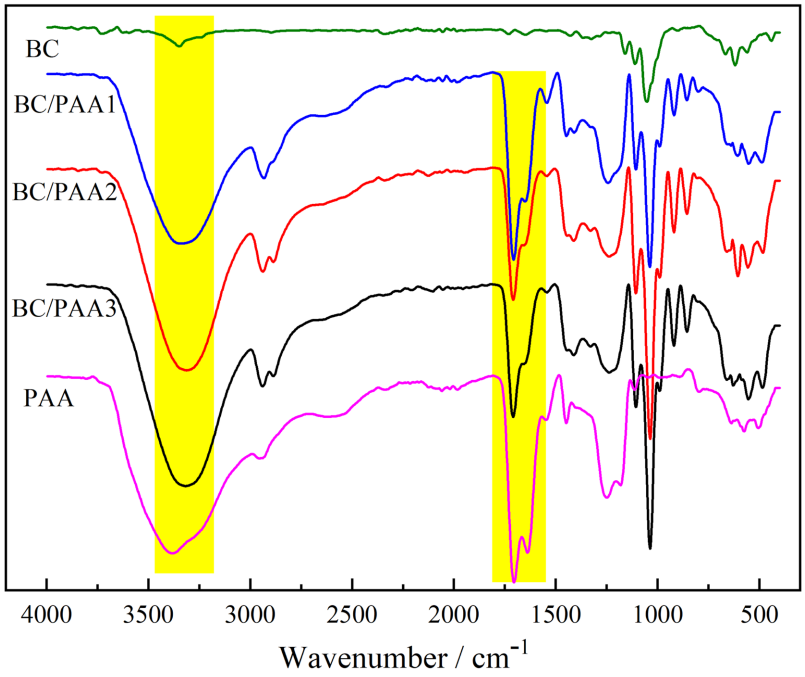

Figure 4. IR spectrum of BC/PAA1, BC/PAA2, BC/PAA3, BC, and PAA.

which was consistent with that of BC at 1051 cm^{-1}, the 907 cm^{-1} and 902 cm^{-1} cyclic C-O-C stretching vibration of BC were consistent with the disappearance of the characteristic C=C absorption peak in BC/PAA at 1590 cm^{-1} to 1635 cm^{-1}, thus indicating the formation of BC/PAA pH-responsive hydrogels by radical polymerization-initiated cross-linking. With the increase of the BC content in the hydrogel preparation, the absorption peaks of the characteristic groups were approximately the same and no new characteristic peaks appeared; however, the peak intensities of the absorption peaks of the characteristic groups were different, which is probably related to the increase of the BC content in the hydrogel.

The BC [22] pattern had three main diffraction peaks at 14˚, 16˚, and 23˚ and the characteristic peaks corresponding to (110), ($\bar{1}10$), and (200) crystal planes (**Figure 5**), which indicate that BC had a cellulose type I crystalline structure. The PAA hydrogel showed no sharp crystallization peak. The peak shape was flat, which indicates that the crystallinity is small. The obvious crystallization peak appeared at 23˚ on the hydrogel curve prepared by BC/PAA, which indicates that the addition of BC could improve the crystallization performance of the BC/PAA pH-responsive hydrogel, which was related to the high crystallinity of BC itself. Furthermore, a large number of hydrogen bonds were established between BC molecules and PAA molecular chains, which further improved the crystallinity of the hydrogel.

PAA hydrogel without BC had a smooth surface and a less porous structure (**Figure 6(a)**). It can be seen from **Figures 6(b)-(d)** that, with the incorporation of BC, the BC/PAA hydrogel forms a loose and porous structure and that there

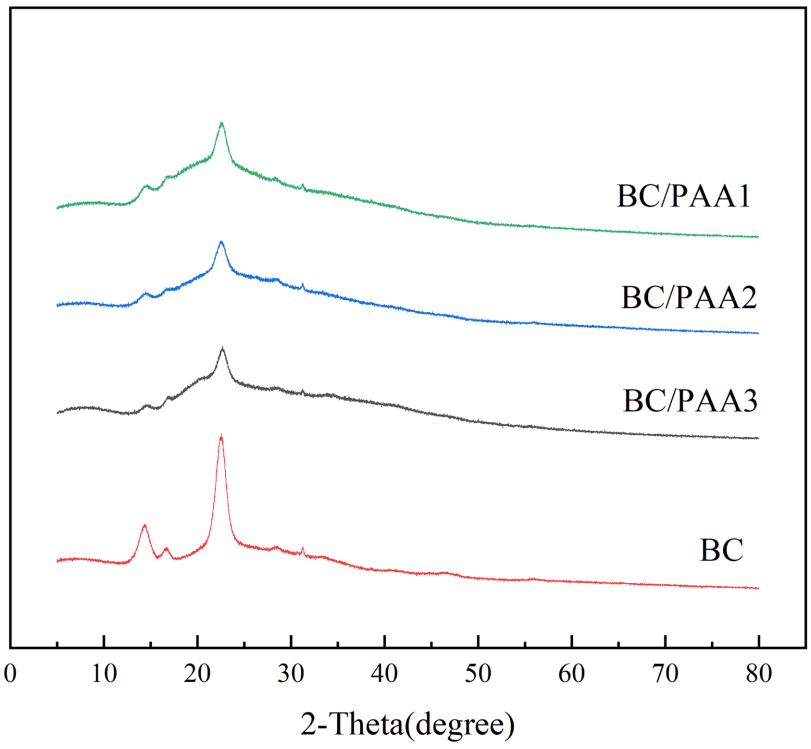

Figure 5. XRD pattern of BC/PAA pH-responsive hydrogel.

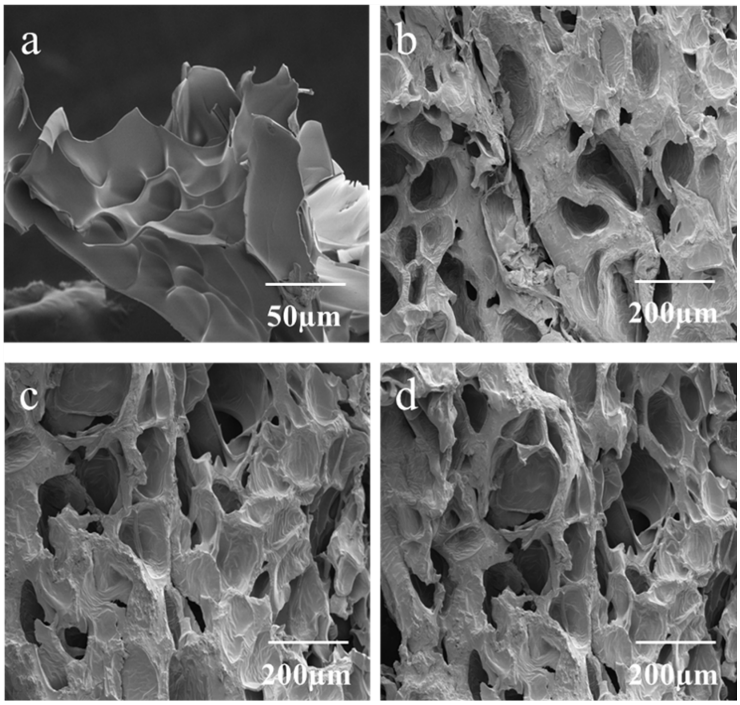

Figure 6. SEM images of PAA (a), BC/PAA1 (b), BC/PAA2 (c), and BC/PAA3 (d).

is a laminar structure of "pore over pore", which has more storage space, makes the composite hydrogel to possess a better swelling and water holding capacity.

The energy storage modulus (G') of the hydrogel characterizes the elastic properties of the sample, while the loss modulus (G") characterizes the flow properties. In the frequency range of 0 - 10 Hz, the G' of the BC/PAA pH-responsive hydrogel with different mass fractions of BC is greater than G", which indicates that the BC/PAA pH-responsive hydrogels possess stable viscoelastic solid properties and are outstanding elastic gels (**Figure 7**). The value of G"/G' is used to refer to the viscoelastic and mechanical properties of a gel [25]. With the gradual increase of the BC content, the G"/G' of each hydrogel sample decreased, which indicates that the crosslinking degree of the hydrogel increased and showed good elastic properties (**Table 3**). BC had a regulatory effect on the elastic properties and mechanical strength of the hydrogel. When m_{AA}/m_{BC} is 3:7 (BC/PAA3), G' could reach 8.6 kPa, thus indicating that the hydrogel had good elasticity and mechanical strength.

A good mechanical property is an important factor in the practical application of hydrogel dressings. If the hydrogel is fragile, it is easily destroyed during application (causing the burst release of the drug), which cannot achieve a good therapeutic effect. As can show in **Table 3**, with the increase of the BC content, the compressive strength of the hydrogels showed an overall upward trend. When m_{AA}/m_{BC} (BC/PAA3) was 3:7, the maximum compressive strength of the hydrogels was 10.3 g/cm^2 and the hydrogels were compressed to 70% of their original height without rupture (**Figure 7(b)**), thus indicating that the prepared hydrogels had high strength and toughness. This is linked to the increase of pore

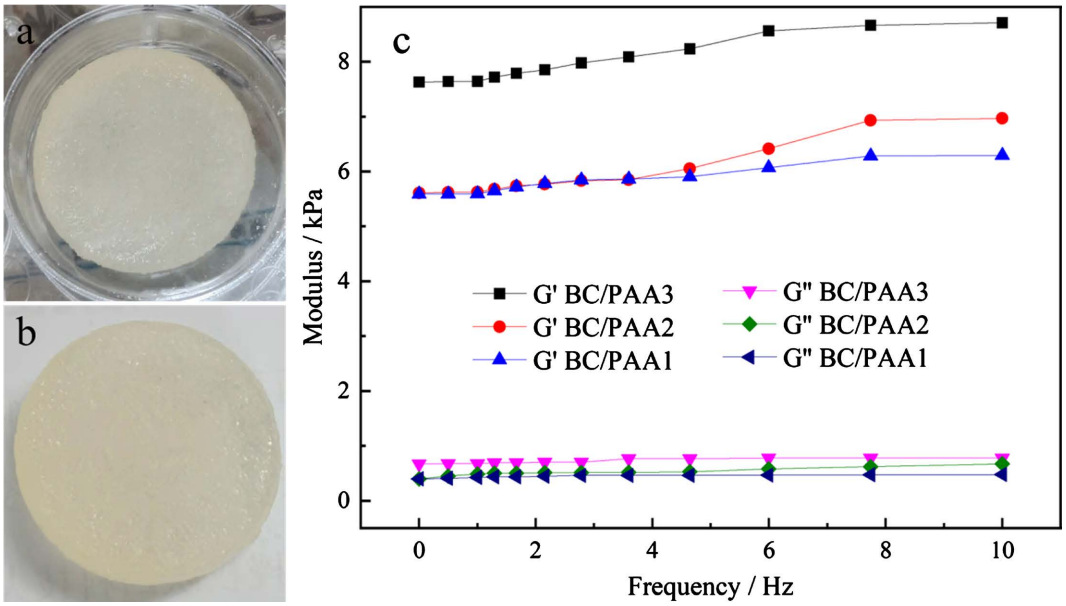

Figure 7. BC/PAA pH-responsive hydrogel with a m_{AA}/m_{BC} of 3:7: before compression (a), after compression (b), and rheological curve (c).

Table 3. Effects of m_{AA}/m_{BC} on G"/G' of BC/PAA pH-responsive hydrogel and its compressive strength.

Sample	BC/PAA1	BC/PAA2	BC/PAA3
G"/G' (at 10 Hz)	0.2459	0.2285	0.1954
Strength(g/cm^2)	1.9	8.6	10.3

and network structure of the hydrogels by BC. From the SEM results in Figure 6, it can be seen that the pores of the hydrogels are more uniform with the addition of BC, which indicates that BC fibers play a supporting role in hydrogels by improving the G' and mechanical properties of hydrogels.

The BC/PAA2 hydrogels showed rapid water absorption properties in different pH solutions and their swelling ratios increased rapidly in a short time. After swelling for 10 h, the swelling rate of the hydrogel was 1200 g/g in pH = 5 (acidic) environment, 1400 g/g in pH = 7 (neutral) environment, and 1600 g/g in the pH = 8 (alkaline) environment (Figure 8), thus indicating that the swelling rate of the BC/PAA pH-responsive hydrogel in the alkaline environment was higher than that in the neutral and acidic environment and that the hydrogel had good pH responsiveness. This is because acrylic acid deprotonates at a pH above its pKa (4.25), leading to a high network osmotic pressure, which results in the expansion of the hydrogel network. However, when the ambient pH is lower than the pKa value of polyacrylic acid, the network structure of polyacrylic acid deprotonates [26] and the solvated polyacrylic acid returns to the protonated state. In an acidic environment, the hydrogel will have a tighter structure due to the stronger hydrogen bond between the carboxyl groups in the acrylic-based hydrogel network structure. However, in alkaline or neutral environments, this

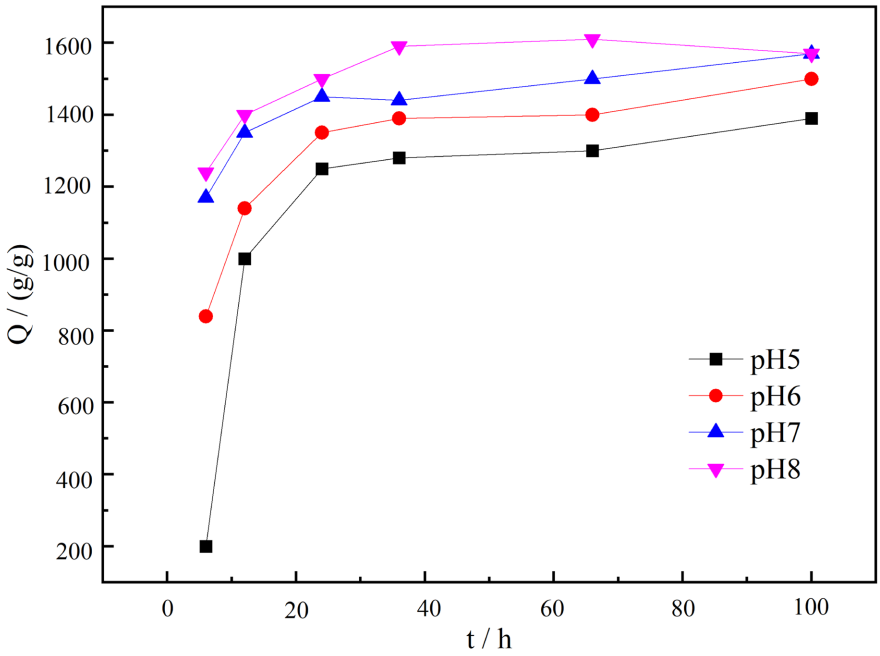

Figure 8. Swelling properties of BC/PAA hydrogels with of mAA/mBC of 1:2 in different pH environments.

hydrogen bonding will be disrupted and electrostatic repulsion occurs between the chain segments in the hydrogel network structure, thus resulting in a hydrogel with a higher swelling rate. The good pH responsiveness of the BC/PAA pH-responsive hydrogel prepared in this study allows the hydrogel to be used as a wound dressing with the ability to respond to pH changes caused by wound infection, thus achieving intelligent drug release and better absorption of wound exudate in ulcer-like wounds treatment.

As depicted in **Figure 9**, the overall trend of Cur release rate in BC/PAA-Cur dressing increased and then leveled off as the release time increased. The drug release rate tended to increase rapidly from 0 to 10 h. In pH = 8 solution, the drug release rate of the BC/PAA-Cur dressing reached a maximum of 57.2% at 60 h. In pH = 4 solution, the BC/PAA-Cur dressing reached a maximum drug release rate of 11.4% at 10 h. This shows that the BC/PAA-Cur dressing possesses good and sustained drug release in an alkaline solution (pH = 8), with a cumulative drug release that is five times higher than that in an acidic environment (pH = 4). This is closely linked to the good pH responsiveness of the hydrogel. Shang et al. proved that, compared with acidic conditions, the pore size and swelling rate of acrylic hydrogel increased in an alkaline environment, which was consistent with the results of this study [27]. The good pH-responsive drug release behavior of the BC/PAA-Cur dressing allows it to maintain a low swelling rate and a tight structure in an acidic environment, where the drug is "protected" inside the hydrogel and where the hydrogel swells further when the environmental pH increases, thus allowing the drug to be released. For chronic bacterial infection wounds, the surface was weakly alkaline (Ph > 7.3). When the

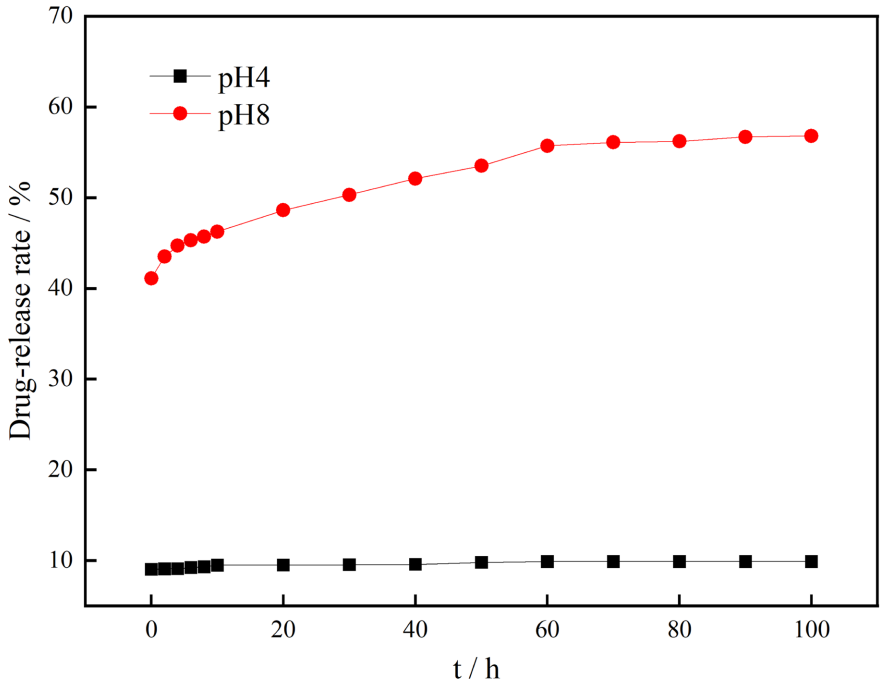

Figure 9. Effect of pH on the release performance of drug-loaded BC/PAA pH-responsive hydrogel.

hydrogel was used in the wound, the drug could be made public at a faster rate, thus killing bacteria in a shorter time. For instance, for pus or necrotic tissue wounds (such as ulcers), the surface of the wound is acidic, which makes the drug release remain low in order to avoid drug abuse when the wound is not infected. Meanwhile, appropriate swelling capacity enables the dressing to exchange pus, blood, and other substances on the wound interface and strengthen wound healing. The above drug release behavior suggests the BC/PAA-Cur dressing as a modern intelligent medical dressing.

Under different pH conditions, with the increase of ionic strength in the drug release environment, the overall Cur release rate showed a tendency of first increase and then became flattered. **Figure 10(a)** showed that the maximum drug release rates of the BC/PAA-Cur dressings in an acidic environment (pH = 4) with C_{NaCl} = 0.11 mol/L, 0.15 mol/L, and 0.17 mol/L were 13.8%, 13.2%, and 12.6%, respectively. **Figure 10(b)** shows that the maximum drug release rates of the BC/PAA-Cur dressing in an alkaline environment (pH = 8) at C_{NaCl} = 0.11 mol/L, 0.15 mol/L, and 0.17 mol/L were 63.2%, 55%, and 49%, respectively. This indicates that the greater the ionic strength, the more unfavorable the release of Cur in the drug-loaded gel becomes, which might be related to the change in osmotic pressure in the release environment. Therefore, when the ionic strength of the tissue fluid increases in the process of skin tissue injury, its effect on Cur release should be considered.

As depicted in **Figure 11**, with an increase in temperature, the overall drug release rate showed an initial increasing trend and then became flattered. In an

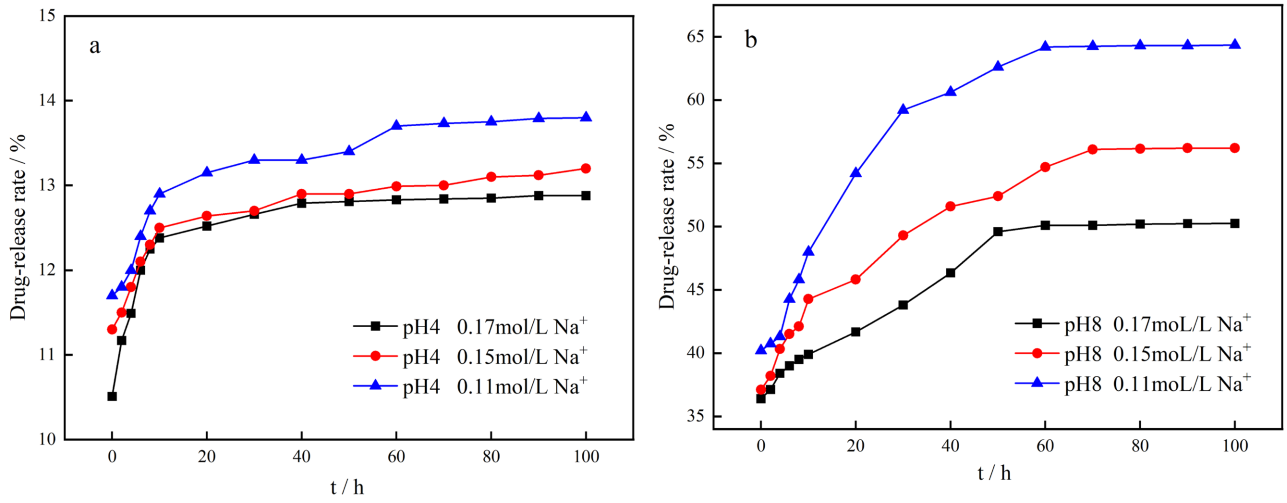

Figure 10. Effect of ionic strength on the pH response of BC/PAA hydrogel ((a) pH 4 PBS, (b) pH 8 PBS).

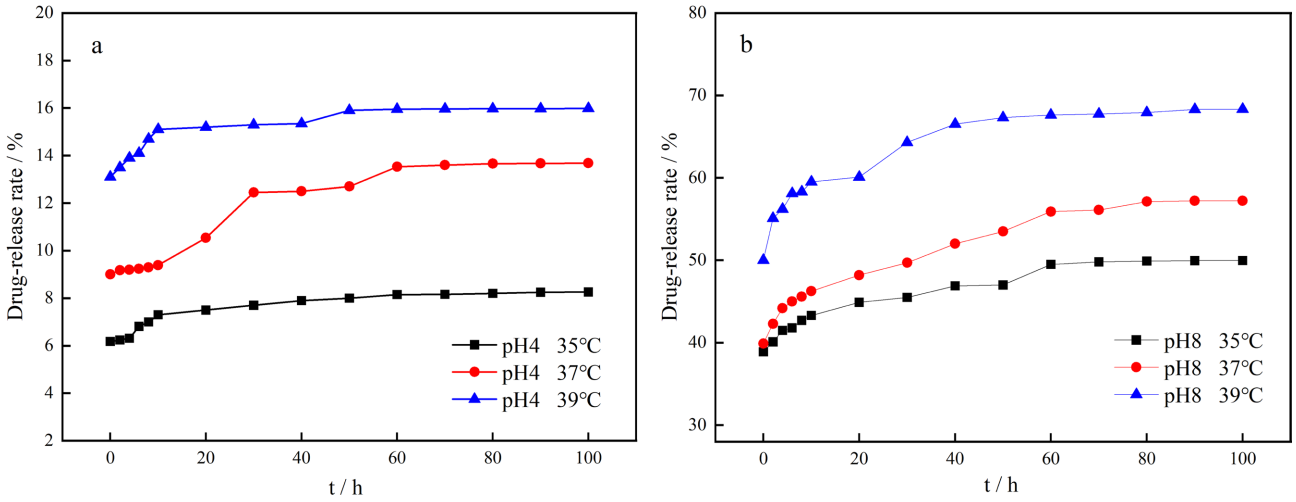

Figure 11. Effect of temperature on the release performance of drug-loaded BC/PAA pH-responsive hydrogel ((c) pH PBS, (d) pH8 PBS).

acidic environment (pH = 4), the drug release rate of the BC/PAA-Cur dressing increased with the increase of temperature; however, the overall drug release rate remained at a low level (the maximum drug release rate was 16% at 39˚C). In an alkaline medium (pH = 8), the BC/PAA-Cur dressing reached the drug release equilibrium at 39˚C for 60 h and the cumulative drug release rate was 70%, while the cumulative drug release rates at 37˚C and 35˚C were 57.3% and 48.1%, respectively. During drug release, as the temperature increases, the rate of Cur molecules diffusion accelerates, and the rate of drug release increases. The beginning phase of drug release is faster, which facilitates the rapid introduction of a higher concentration of the drug locally in the wound, thus effectively controlling the infection [28]. In the subsequent phase, the drug is released slowly and continuously for several hours, which can be tailored to the long-term control of infection.

In this study: 1) the Zero-level release model $Q = a + bx$ [29]; 2) the Higuchi

equation $Q = bx^{1/2} + a$ [30]; 3) the Logistic equation $Q = a + (b - a)/(1 + (x/c)^d$ [31]; and 4) the SWeibull equation $Q = a-(a - b)e^{-(kx)^{\wedge}d}$ (Q is the cumulative release rate, X is the release time, and a, b, c, d, and k are the fitting constants) [32] were applied. The release curves of the BC/PAA-Cur dressing in PBS solutions at pH = 4 and pH = 8 were fitted. The fitting curves and kinetic equations are illustrated in **Figure 12** and **Table 4**. Compared with the zero-level release model, the kinetic model of Cur release from the BC/PAA-Cur dressing under different pH conditions established by the logistic kinetic model was well-fitted and the R^2 was greater than 0.9800, thus indicating that the kinetic behavior of Cur release from the BC/PAA-Cur dressing under different conditions can be described by the logistic kinetic model. The Higuchi and Sweibull models can both be well-fitted for the Cur release process. The basic material of the BC/PAA-Cur dressing BC has a nice three-dimensional network structure and the hydrogel prepared by BC/PAA-Cur has a large number of network pore structures itself. During the drug loading process, Cur cannot only partially be adsorbed on the

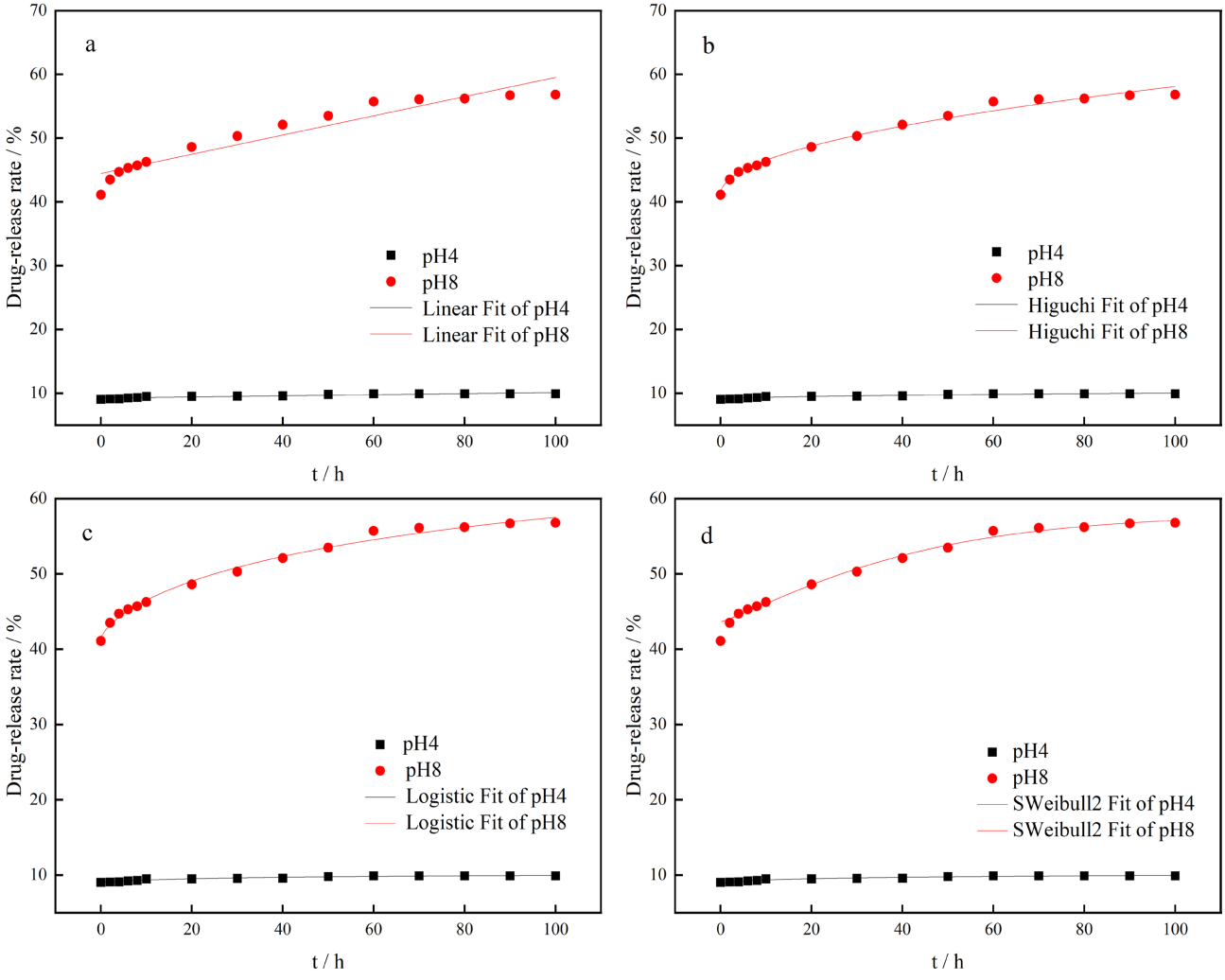

Figure 12. Drug release kinetics fitting curves of BC/PAA pH-responsive hydrogels in pH 4 and pH 8 PBS (a) the zero-level dynamics; (b) the Higuchi dynamics; (c) the logistic dynamics; and (d) the SWeibull dynamics.

surface of the hydrogel but can enter the hydrogel pore structure and be wrapped by the gel pore, thereby forming a skeleton drug loading system. Therefore, the Higuchi and Sweibull models can both be used to better describe the Cur release kinetics of the BC/PAA-Cur dressing. Among them, the logistic kinetic equation can better describe the release behavior of the BC/PAA-Cur dressing, and its actual cumulative release curve overlaps well with the fitted curve, thus indicating that the release mechanism under this condition is not just a simple process of diffusion but with hysteresis, mutation, and complete release.

Figure 13(a) showed that the indicator bacteria without BC/PAA-Cur pH-responsive hydrogel incubation appeared in a large number of colonies after plating the culture. While the indicator bacteria incubated with BC/PAA-Cur2, BC/PAA-Cur3, and BC/PAA-Cur6 showed a decreasing trend after plating the culture. According to the quantitative analysis of the colony number (Figure 13(b)),

Table 4. Dynamic fitting of the drug release process.

Sample	model	equation	R^2
	Zero-level	$Q = 0.0087t + 9.2124$	0.83618
	Higuchi	$Q = 0.09953t1/2 + 9.0162$	0.93846
pH4	Logistic	$Q = 10.2831.2765/(1 + \frac{t}{32.431})0.8855$	0.98928
	SWeibull	$Q = 10.5191 - 10.5191\exp(-0.01579t0.3911)$	0.94121
	Zero-level	$Q = 0.1507t + 44.4426$	0.9073
	Higuchi	$Q = 1.68901t1/2 + 41.19153$	0.97934
pH8	Logistic	$Q = 0.38439 - 0.31355/(1 + \frac{t}{24.0552})0.30118$	0.9897
	SWeibull	$Q = 57.9239 - 57.9239\exp(0.02408t1.18857)$	0.99312

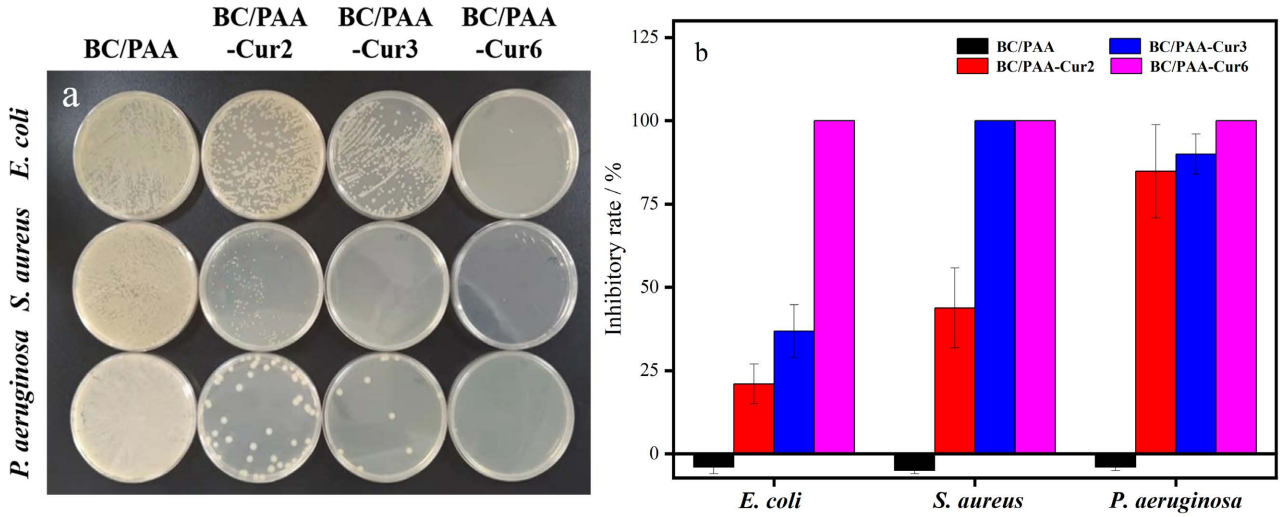

Figure 13. (a) Antibacterial property of hydrogels using agar diffusion assay; (b) Antibacterial effect of hydrogels on *E. coil*, *S. aureus*, and *P. aeruginosa*.

the inhibition rates of BC/PAA-Cur6 against *E. coil*, *S. aureus*, and *P. aeruginosa* were 96.53%, 99.73%, and 94.24%, respectively, which indicates that the BC/PAA-Cur dressing had good antibacterial properties against *E. coil*, *S. aureus*, and *P. aeruginosa*. With the increase of the Cur content, the antibacterial ability increased, which indicates that the drugs in the dressing could be effectively released and that the drugs had good antibacterial properties.

The cell membrane is a major structural component of bacteria and intracellular biochemical reactions and respiration are closely related to it. In order to clarify the antibacterial potential mechanism of the BC/PAA-Cur dressing, the calcein-AM/PI double fluorescence staining method was used to evaluate the integrity of the indicator bacteria cell membrane after the dressing treatment. Calcein-AM is cleaved by intracellular esterases to form the membrane-impermeable polar molecule calcein, which is retained in cells and emits strong green fluorescence (liver cells). PI cannot cross the membrane of living cells but can pass through disordered regions of the membrane of dead cells to reach the nucleus and intercalate into the DNA double helix of the cell to produce red fluorescence (dead cells).

After 12 h of co-culture of the bacteria and materials, *E. coil*, *S. aureus*, and *P. aeruginosa* treated with the BC/PAA pH-responsive hydrogel showed green fluorescence under LSCM (**Figure 14**); however, for the strains treated with BC/PAA-Cur dressing, red fluorescence was observed to increase from less to more with increasing drug concentration under LSCM. This indicates that the BC/PAA-Cur dressing can kill bacteria by disrupting the bacterial cell membrane.

The SEM of *E. coil*, *S. aureus*, and *P. aeruginosa* after incubation with BC/PAA pH-responsive hydrogel and BC/PAA/Cur-3 are shown in **Figure 15**. After incubation in the hydrogel without Cur loading, *E. coil*, *S. aureus*, and *P. aeruginosa* on BC/PAA hydrogel were rod-shaped and spherical and had smooth surfaces. After the BC/PAA/Cur-3 treatment, a large amount of intracellular leakage from the surface of *P. aeruginosa* could be observed. Also, the morphology of *E. coil* and *S. aureus* was significantly damaged, with the surface wrinkled, distorted,

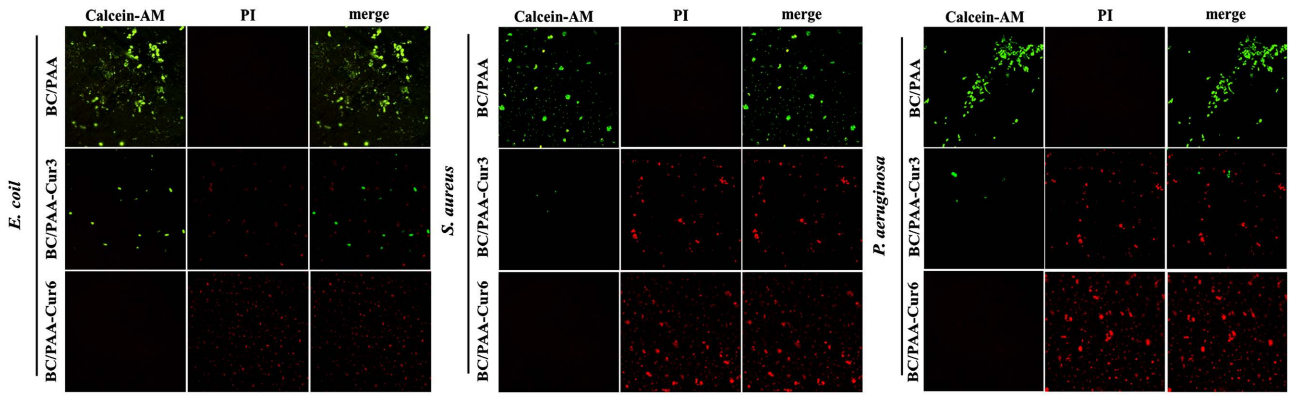

Figure 14. Confocal images of the three bacterial strains with calcein-AM/PI dual fluorescent staining after 12 h of co-incubation with different hydrogels.

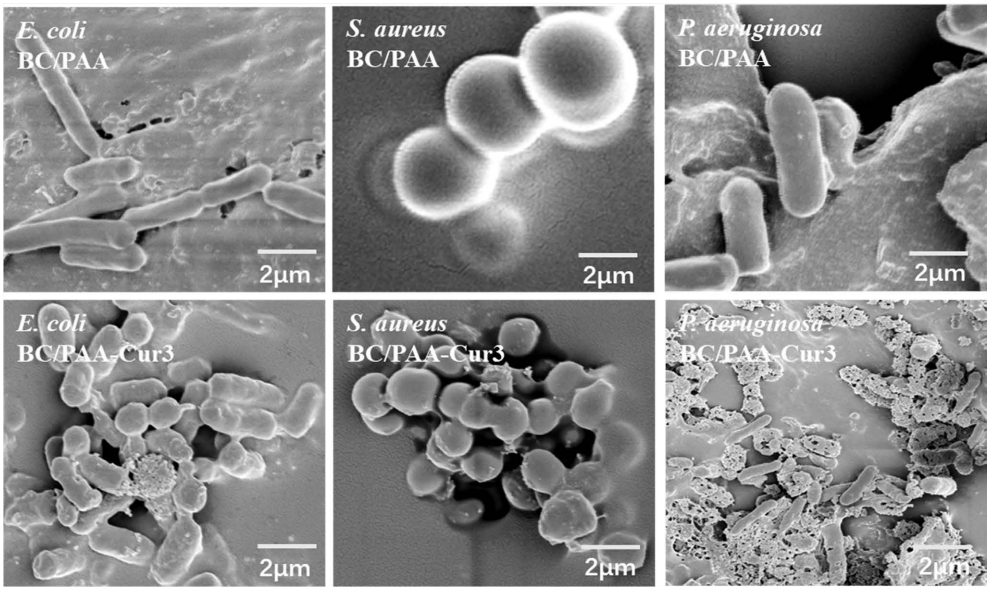

Figure 15. SEM images of the morphology of *E. coli*, *S. aureus*, and *P. aeruginosa* after 12 h of co-incubation with BC/PAA and BC/PAACur-3 hydrogels.

and no longer intact. Studies have shown that Cur may destroy the cell membrane or break *E. coil* cells through a special mechanism. Wang et al. reported that Cur has antibacterial activity against *S. aureus* and that the mechanism is through the destruction of the bacterial cell wall, followed by its spread into the cell and destruction of cellular organelle structure, thus eventually leading to apoptosis [33]. Similarly, Yun and Lee [34] reported in their study that Cur induces the production and intracellular accumulation of reactive oxygen species, which in turn damages macromolecules, such as proteins, nucleic acids (DNA/RNA), and lipid membranes, thereby leading to apoptosis. It is suggested that Cur may induce cell death through any of the above mechanisms. These results suggest that the combination of Cur and pH-responsive hydrogels can be used as a smart antimicrobial wound dressing to treat local skin injuries.

4. Conclusions

1) The optimal preparation process of pH-responsive hydrogel is as follows: a reaction temperature of 65˚C, reaction time of 30 min, BC/PAA mass ratio of 2:1, 0.025% initiator, and 0.5% cross-linking agent. The hydrogel swelling rate prepared under this process can reach 1600 g/g. The prepared BC/PAA pH-responsive hydrogel has a three-dimensional network structure, which can achieve rapid release or sustained release of drugs by adjusting pH. The dissolution rate increases from 200 g/g to 1600 g/g within 48 h at pH = 5 - 8.

2) The compressive strength of the pH-responsive hydrogel can reach up to 8.7 kPa, with good mechanical properties. The storage modulus of the hydrogel is about (1 - 30) × 10^3 Pa under the shear action of 0.01 - 1.00 rad/min and the mechanical properties are stable.

3) The drug release behavior of the BC/PAA-Cur dressing prepared based on

the pH-responsive hydrogel conforms to the logistic kinetic model, showing good wound pH responsiveness, sustained drug release characteristics, and antibacterial activity against common pathogens, such as *E. coil*, *S. aureus*, and *P. aeruginosa*, by damaging the bacterial cell membrane. The findings from this study provide a foundation for the development of new medical dressings that have good economic and social benefits in the modern pharmaceutical industry.

In the future, the pharmacodynamics of the dressing will be evaluated, animal skin wound models will be established, and the wound healing effect of the dressing will be studied at the cellular level and molecular level to clarify the practical application of the dressing in wound healing and to lay the foundation for its practical application as a medical dressing.

Acknowledgements

The research was funded by Key Laboratory of Wuliangye-flavor Liquor Solid-state Fermentation, China National Light Industry (Program No. 2019JJ011), Solid-state Fermentation Resource Utilization Key Laboratory of Sichuan Province (Program No. 2019GTJ006), Xi'an Science and Technology Planning Project (Program No. 21XJZZ0002), and Xi'an Weiyang District Science and Technology Plan (Program No. 202130).

Conflicts of Interest

The authors declare no conflicts of interest regarding the publication of this paper.

References

[1] Yeo, D.C., Chew, S.W.T. and Xu, C.J. (2019) Polymeric Biomaterials for Management of Pathological Scarring. *ACS Applied Polymer Materials*, **1**, 612-624. https://doi.org/10.1021/acsapm.8b00203

[2] Shi, M., Zhang, H., Song, T., Liu, X.F., Gao, Y.F. and Zhou, G.H. (2019) Sustainable Dual Release of Antibiotic and Growth Factor from pH-Responsive Uniform Alginate Composite Microparticles to Enhance Wound Healing. *ACS Applied Materials & Interfaces*, **11**, 22730-22744. https://doi.org/10.1021/acsami.9b04750

[3] Jiang, M.Y., Ju, X.J., Lu, F., Liu, Z., Wang, W., Xie, R., Chen, Q., *et al*. (2014) A Novel Smart Microsphere with K^+-Induced Shrinking and Aggregating Property Based on Responsive Host-Guest System. *ACS Applied Materials & Interfaces*, **6**, 19405-19415. https://doi.org/10.1021/am505506v

[4] Zhong, Y., Xiao, H., Seidi, F. and Jin, Y.C. (2020) Natural Polymer-Based Antimicrobial Hydrogels without Synthetic Antibiotics as Wound Dressings. *Biomacromolecules*, **21**, 2983-3006. https://doi.org/10.1021/acs.biomac.0c00760

[5] Xu, C., Akakuru, O.U., Ma, X.H., Zheng, J.P., Zheng, J.J. and Wu, A. (2020) Nanoparticle-Based Wound Dressing: Recent Progress in the Detection and Therapy of Bacterial Infections. *Bioconjugate Chemistry*, **31**, 1708-1723. https://doi.org/10.1021/acs.bioconjchem.0c00297

[6] Memic, A., Abudula, T., Mohammed, H.S., Navare, J.K. and Colombani, T. (2019) Latest Progress in Electrospun Nanofibers for Wound Healing Applications. *ACS Applied Bio Materials*, **2**, 952-969. https://doi.org/10.1021/acsabm.8b00637

[7] Wu, H., Li, F.Y., Shao, W., Gao, J.Q. and Ling, D.S. (2019) Promoting Angiogenesis in Oxidative Diabetic Wound Microenvironment Using a Nanozyme-Reinforced Self-Protecting Hydrogel. *ACS Center Science*, **5**, 477-485. https://doi.org/10.1021/acscentsci.8b00850

[8] Xie, J.B. and Hsieh, Y.-L. (2003) Thermosensitive Poly(N-Isopropylacrylamide) Hydrogels Bonded on Cellulose Supports. *Journal of Applied Polymer Science*, **89**, 999-1006. https://doi.org/10.1002/app.12206

[9] Shao, W., Liu, H., Liu, X.F., Wang, S.X. and Zhang, R. (2015) Anti-Bacterial Performances and Biocompatibility of Bacterial Cellulose/Graphene Oxide Composites. *RSC Advances*, **5**, 4795-4803. https://doi.org/10.1039/C4RA13057J

[10] Sajjad, W., He, F., Ullah, M.W., Ikre, M., Shah, S.M., Khan, T., *et al*. (2020) Fabrication of Bacterial Cellulose-Curcumin Nanocomposite as a Novel Dressing for Partial Thickness Skin Burn. *Frontiers in Bioengineering and Biotechnology*, **8**, Article 553037. https://doi.org/10.3389/fbioe.2020.553037

[11] Lee, S.E. and Park, Y.S. (2017) The Role of Bacterial Cellulose in Artificial Blood Vessels. *Molecular & Cellular Toxicology*, **13**, 257-261. https://doi.org/10.1007/s13273-017-0028-3

[12] Zheng, L., Li, S.S., Luo, J. and Wang, X.Y. (2020) Latest Advances on Bacterial Cellulose-Based Antibacterial Materials as Wound Dressings. *Frontiers in Bioengineering and Biotechnology*, **8**, Article 593768. https://doi.org/10.3389/fbioe.2020.593768

[13] Jalababu, R., Satya, S., Veni, S. and Reddy, K.V.N.S. (2019) Development, Characterization, Swelling, and Network Parameters of Amino Acid Grafted Guar Gum Based pH Responsive Polymeric Hydrogels. *International Journal of Polymer Analysis and Characterization*, **24**, 304-312. https://doi.org/10.1080/1023666X.2019.1594058

[14] Mao, L., Wang, L., Zhang, Y.M., Ullah, W.M., Zhao, W.W. and Li, Y. (2021) *In Situ* Synthesized Selenium Nanoparticles-Decorated Bacterial Cellulose/Gelatin Hydrogel with Enhanced Antibacterial, Antioxidant, and Anti-Inflammatory Capabilities for Facilitating Skin Wound Healing. *Advanced Healthcare Materials*, **10**, e2100402. https://doi.org/10.1002/adhm.202100402

[15] Zhang, Z.Y., Sun, Y., Zheng, Y.D., He, W., Yang, Y.Y., Xie, J.Y., *et al*. (2020) A Biocompatible Bacterial Cellulose/Tannic Acid Composite with Antibacterial and Anti-Biofilm Activities for Biomedical Applications. *Materials Science Engineering*: *C*, **106**, Article ID: 110249. https://doi.org/10.1016/j.msec.2019.110249

[16] Ahmad, N., Amin, M.C., Mahali, S.M., Ismail, I. and Chuang, G.T.V. (2014) Biocompatible and Mucoadhesive Bacterial Cellulose-g-Poly(Acrylic Acid) Hydrogels for Oral Protein Delivery. *Molecular Pharmaceutics*, **11**, 4130-4143. https://doi.org/10.1021/mp5003015

[17] Zhang, H., Tang, N., Yu, X., Guo, Z.K., Liu, Z. and Sun, X.M. (2022) Natural Glycyrrhizic Acid-Tailored Hydrogel with *In-Situ* Gradient Reduction of AgNPs Layer as High-Performance, Multi-Functional, Sustainable Flexible Sensors. *Chemical Engineering Journal,* **430**, Article ID: 132779. https://doi.org/10.1016/j.cej.2021.132779

[18] Napavichayanun, S., Ampawong, S., Harnsilpong, T., Angspatt, A., Aramwit, P. (2018) Inflammatory Reaction, Clinical Efficacy, and Safety of Bacterial Cellulose Wound Dressing Containing Silk Sericin and Polyhexamethylene Biguanide for Wound Treatment. *Archives of Dermatological Research,* **310**, 795-805. https://doi.org/10.1007/s00403-018-1871-3

[19] Rueda, J.C., Suarez, C., Komber, H., Zschoche, S. and Voit, B. (2020) Synthesis and Characterization of pH- and Thermo-Responsive Hydrogels Based on Poly(2-Cyclopropyl-2-Oxazoline) Macromonomer, Sodium Acrylate, and Acrylamide. *Polymer Bulletin*, **77**, 5553-5565. https://doi.org/10.1007/s00289-019-03034-0

[20] Warune, T., Jate, P. and Sayant, S. (2019) Novel Biodegradable Hydrogel Based on Natural Polymers: Synthesis, Characterization Swelling/Reswelling and Biodegradability. *European Polymer Journal*, **112**, 678-687. https://doi.org/10.1016/j.eurpolymj.2018.10.033

[21] Cristiane, S., Francisco, H.A.R., Antonio, G.B.P., André, R.F., Adley, F.R. and Edvani, C.M. (2012) Superabsorbent Hydrogel Composite Made of Cellulose Nanofibrils and Chitosan-Graft-Poly(Acrylic Acid). *Carbohydrate Polymers*, **87**, 2038-2045. https://doi.org/10.1016/j.carbpol.2011.10.017

[22] Sajjad, W., He, F., Ullah, M.W., Ikram, M., Shah, S.S., Khan, R., *et al*. (2020) Fabrication of Bacterial Cellulose-Curcumin Nanocomposite as a Novel Dressing for Partial Thickness Skin Burn. *Frontiers in Bioengineering and Bioengineering,* **8**, Article 553037. https://doi.org/10.3389/fbioe.2020.553037

[23] Chen, X.Y., Low, H.R., Loi, X.Y., Merel, L. and Iqbal, M.A.M.C. (2019) Fabrication and Evaluation of Bacterial Nanocellulose/Poly(Acrylic Acid)/Graphene Oxide Composite Hydrogel: Characterizations and Biocompatibility Studies for Wound Dressing. *Journal of Biomedical Materials Research Part B*: *Applied Biomaterials*, **107**, 2140-2151. https://doi.org/10.1002/jbm.b.34309

[24] Amin, M.C.I.M., Ahmad, N., Halib, N. and Ahmad, I. (2012) Synthesis and Characterization of Thermo and pH-Responsive Bacterial Cellulose/Acrylic Acid Hydrogels for Drug Delivery. *Carbohydrate Polymers*, **88**, 465-473. https://doi.org/10.1016/j.carbpol.2011.12.022

[25] Ozay, O. (2014) Synthesis and Swelling Behavior of Novel pH Responsive Hydrogels for Environmental Applications. *Polymer-Plastics Technology and Engineering*, **53**, 130-140. https://doi.org/10.1080/03602559.2013.843697

[26] Zhang, X., Meng, Y., Shen, W., Dou, J.C., Liu, R., *et al*. (2021) pH-Responsive Injectable Polysaccharide Hydrogels with Self-Healing, Enhanced Mechanical Properties Based on POSS. *Reactive and Functional Polymers*, **158**, Article ID: 104773. https://doi.org/10.1016/j.reactfunctpolym.2020.104773

[27] Shang, J.J. and Theato, P. (2018) Smart Composite Hydrogel with pH-, Ionic Strength- and Temperature-Induced Actuation. *Soft Matter*, **14**, 8401-8407. https://doi.org/10.1039/C8SM01728J

[28] Sun, L., Wang, Y., Jiang, T.Y., Zheng, X., Zhang, H.J., Sun, J. and Sun, C.S. (2013) A Novel Chitosan Functionalized Spherical Nanosilica Matrix as a Sustained Drug Delivery System for the Poorly Water-Soluble Drug Carvedilol. *ACS Applied Materials & Interfaces*, **5**, 103-113. https://doi.org/10.1021/am302246s

[29] Korsmeyer, R.W., Gumy, R., Doelker, E., Buri, P. and Peppas, N.A. (1983) Mechanisms of Solute Release from Porous Hydrophilic Polymers. *International Journal of Pharmaceutics*, **15**, 25-35. https://doi.org/10.1016/0378-5173(83)90064-9

[30] Higuchi, T. (1963) Mechanism of Sustained-Action Medication. Theoretical Analysis of Rate of Release of Solid Drugs Dispersed in Solid Matrices. *Journal of Pharmaceutical Sciences*, **52**, 1145-1149. https://doi.org/10.1002/jps.2600521210

[31] Berry, M.R. and Likar, M.D. (2007) Statistical Assessment of Dissolution and Drug Release Profile Similarity Using a Model-Dependent Approach. *Journal of Pharmaceutical and Biomedical Analysis*, **45**, 194-200. https://doi.org/10.1016/j.jpba.2007.05.021

[32] Van Boekel, M.A.J.S. (2002) On the Use of the Weibull Model to Describe Thermal Inactivation of Microbial Vegetative Cells. *International Journal of Food Microbiology*, **74**, 139-159. https://doi.org/10.1016/S0168-1605(01)00742-5

[33] Wang, H., Hao, L., Wang, P., Chen, M., Jiang, S.W. and Jiang, S.T. (2016) Release Kinetics and Antibacterial Activity of Curcumin Loaded Zein Fibers. *Food Hydrocolloids*, **63**, 437-446. https://doi.org/10.1016/j.foodhyd.2016.09.028

[34] Yun, D.G. and Lee, D.G. (2016) Antibacterial Activity of Curcumin via Apoptosis-Like Response in *Escherichia coli*. *Applied Microbiology and Biotechnology*, **100**, 5505-5514. https://doi.org/10.1007/s00253-016-7415-x